THREE-DIMENSIONAL SIMULATION OF A HARMONIC LASING FREE-ELECTRON LASER AMPLIFIER

E. Salehi, B. Maraghechi

Department of Physics, Amirkabir University of Technology, Tehran, Iran,

N.S. Mirian*

UVSOR Facility, Institute for Molecular Science, Okazaki, Japan and
School of Particle and Accelerator Physics, IPM, Tehran, Iran

Abstract

Three-dimensional simulation of harmonic lasing Free-electron laser is represented in the steady-state regime. Here, the third harmonic of the first wiggler is adjusted at the fundamental resonance of the second wiggler by reducing the magnetic field strength of the second wiggler. The hyperbolic wave equations can be transformed into parabolic diffusion equations by using the slowly varying envelope approximation. A set of coupled nonlinear first-order differential equations describing the nonlinear evolution of the system is solved numerically by CYRUS3D code. This set of equations describes self-consistently the longitudinal spatial dependence of the radiation waists, curvatures, and amplitudes together with the evaluation of the electron beam. Thermal effects in the form of longitudinal velocity spread are also investigated.

INTRODUCTION

High-gain free electron laser (FEL) amplifiers hold great prospects of reaching coherent high power radiation in the x-ray region of the electromagnetic spectrum. In recent years, a great effort of researchers has been devoted to studying the process of higher harmonic generation in achieving lasing at shorter wavelengths [1–5].

Radiation of the electron beam in the planar wiggler contains odd harmonics but the output power at the hth harmonics is rather small and is of the order of 10^{-h} times the power of the fundamental [1, 3–5]. Recently, McNeil et al. [6] proposed a harmonic lasing method for FEL amplifiers that can amplify the higher harmonics by suppressing the interaction at the fundamental resonance. They showed that this configuration can significantly extend the operation band of user facilities.

Reference [6] has outlined two methods for suppressing the interaction at the fundamental resonance while allowing the third harmonic to evolve to saturation. The first method is based upon shifting the phase of the fundamental between the wiggler segments, which can be controlled by various techniques [7]. For the hth harmonic, this phase shift should be $2\pi n/h$, where $n = 1, 2, 3, \ldots$ is an integer number and $h = 3, 5, 7, \ldots$ is the harmonic number. The second method is detuning of the fundamental by considering two different segments for the wiggler. Two segments of the wiggler have different magnetic field intensity while the wiggler period,

---

* nsmirian@ims.ac.jp

λ_w, and the initial average electron beam energy, γ, are kept constant.

The thermal effect of the electron beam is particularly important for higher harmonics, because they are more sensitive to the energy spread than the fundamental one [8, 9]. The energy spread is considered as a Gaussian energy distribution in MEDUSA code for nonlinear harmonic generation [10]. Also, in reference [7], the energy spread effects are included that the gain length for the detuning of the fundamental is compared with the third harmonic in conventional FEL.

The aim of this paper is to present a three-dimensional simulation of the emission at the fundamental and third harmonic in the non-wiggler-averaged-orbit approximation of the harmonic lasing FEL with source-dependent expansion [11–14]. Therefore, the source function is incorporated self-consistently into the functional dependence of the radiation waist, the radiation wavefront curvature, and the radiation amplitude instead of using the usual modal expansion consisting of vacuum Laguerre-Gaussian or Hermite-Gaussian functions. It is important to emphasize that no wiggler average is imposed on the orbit equations. Therefore, It is possible to treat the injection of the beam into the wiggler, with the ease of inclusion of external focusing or dispersive magnetic components in the beam line and the facility for using an actual magnetic field in the numerical solution. The third harmonic lasing is considered so that the operating wavelength is in the EUV domain. The slippage of the radiation with respect to the long electron bunch is ignored.

The code which is written for this purpose is named CYRUS 3D, which was developed by PhD students in Amirkabir University and Institute for Research in Fundamental Sciences (IPM). This code follows MEDUSA 3D [10] formulation.

DESCRIPTION OF THE SIMULATION CODE

The simulation code for three-dimensional non-wiggler averaged-orbit formulation is CYRUS 3D code, that was written in standard Fortran 95. This code is time independent with harmonics and thermal effects taken into account. It models planar wiggler and the electromagnetic field is represented as a superposition of Gauss-Hermit modes in the slowly varying amplitude approximation. Electron trajectories are integrated using the three-dimensional(3D) Lorentz

force equations in the magnetostatic and electromagnetic fields.

This code like MEDUSA 3D employs nonaverage equations. The details of the formulation is explained in Ref. [10]. We simulate harmonic lasing FEL in which the wiggler consists of two segments. In the harmonic lasing FEL the wiggler segments have two different magnetic field strengths but the same wavelength λ_w.

The thermal effect of the electron beam on the harmonic gain is particularly important. Higher harmonics are more sensitive to the energy spread than the fundamental one [4, 6, 8]. It was concluded in Ref. [6] that harmonic lasing with phase shifting is more sensitive to the emittance and the energy spread than the harmonic lasing with detuning of the fundamental. In Refs. [15], a spread in the traverse momentum with constant total energy is considered. They showed that a longitudinal spread is more effective than a transverse spread in reducing the growth rate.

To consider effects of the energy spread, we assume longitudinal spread without any spread in the transverse momentum. So, the initial conditions is chosen to model the axial injection of the electron beam with the energy in the form of a Gaussian distribution function that is peaked around the initial energy of the beam. We choose the thermal distribution function as

$$G_0(p_z) \quad = \quad \sqrt{\frac{2}{\pi}} \frac{1}{\Delta p_z} exp\left(-\frac{2(p_z - p_{z0})}{\Delta p_{z^2}}\right), \quad (1)$$

where p_0 and Δp_{z0} are the initial bulk momentum and momentum spread, respectively.

$$\langle(\cdots)\rangle = \int\frac{d\psi_0}{2\pi}\sigma_\parallel(\psi_0)\iint dx_0 dy_0 \sigma_\perp(x_0, y_0)\int dp G_0(p_z)(\cdots) \quad (2)$$

To consider harmonic lasing FEL using the retuned fundamental resonant wavelength, the wiggler is composed of two segments and the wavelength of the fundamental resonance of the second segment is decreased by reducing the magnetic field strength of the second segment of the wiggler. In this case, for the first segment, the rms wiggler parameter is a_1 and the fundamental resonant wavelength is λ_1 giving the harmonic resonant wavelengths as $\lambda_h = \lambda_1/h$, $h = 3, 5, 7, \ldots$. In the second segment, the rms wiggler parameter is reset to a_n so that the new resonant fundamental wavelength is the nth harmonic of the first segment, $\lambda'_1 = \lambda_n$. For the assumed fixed beam energy and wiggler period, the retuned wiggler parameter a_n is obtain from the FEL resonance relation

$$\frac{1 + a_1^2}{1 + a_n^2} = n. \quad (3)$$

Obviously, a_1 must be larger than $a_c = \sqrt{n-1}$. Because there are no real solutions for a_n for $a_1 < a_c$. So, the wiggler can not be reduced to a fundamental wavelength $\lambda'_1 = \lambda_n$ for $a_1 < a_c$. We consider tuning the harmonic interaction
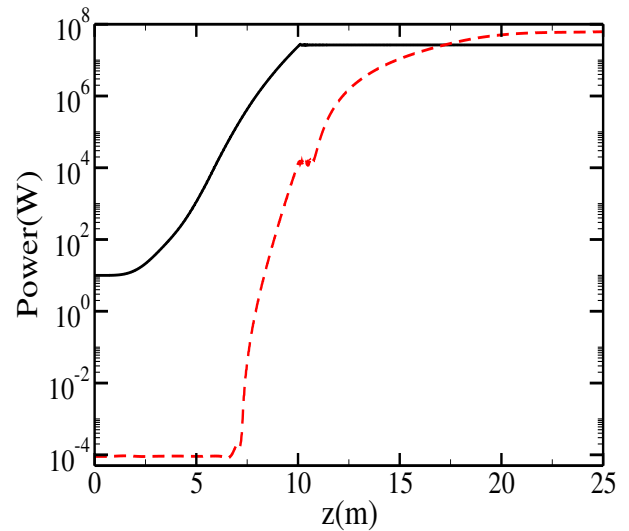
Figure 1: Evolution for the power for the fudamental resonance (solid line) and the third harmonic (dashed line).

by decreasing the wiggler magnetic field; it is clear this is impractical for an operating X-ray FEL.

NUMERICAL ANALYSIS

Self-consistent first-order nonlinear differential equations are solved numerically using the forth-order Runge-Kutta algorithm subject to the appropriate initial conditions and in the time independent approximation where the pulse length is much longer than the slippage length over the course of the wiggler. The particle averages are carried out using a Gaussian quadrature technique in each of the degrees of freedom ($x_0, y_0, \psi_0, \varphi_0, p_{z0}, \gamma_0$). The number of Gauss-Hermite modes that are needed in the code depends on each particular example. The self-guiding effects of the electron beam in an FEL during exponential gain become dominant over the diffraction, and the balance depends on the Rayleigh length, the growth rate, and the evolution of the beam envelope. Therefore, it is necessary to choose a suitable basis set in order to determine the optical mode content. The number of modes that are determined by an empirical procedure in which successive simulation runs are made with an increasing number of modes until convergence of the saturation power and saturation length are achieved.

The parameters for the electron beam, the wiggler, and the radiation in the simulation are as follows. The electron beam has the relativistic factor of 964, a peak current of 300 A, an initial radius of 0.01495 cm, and an energy spread of 0.01%. The wiggler period is 3.3 cm and exhibits a peak of on-axis amplitude equal to 10.06 kG. An entry taper region is $N_w = 10$ wiggler period in length which is necessary in order to inject the electrons into the steady-state trajectories. Using these beams and wiggler parameters, the fundamental resonance is at a wavelength of 102.9 nm in the 1D resonance formula. Because of betatron motion in three dimensions, fundamental resonance is found at the wavelength of 103.6 nm, which is seeded with a 10 W of optical
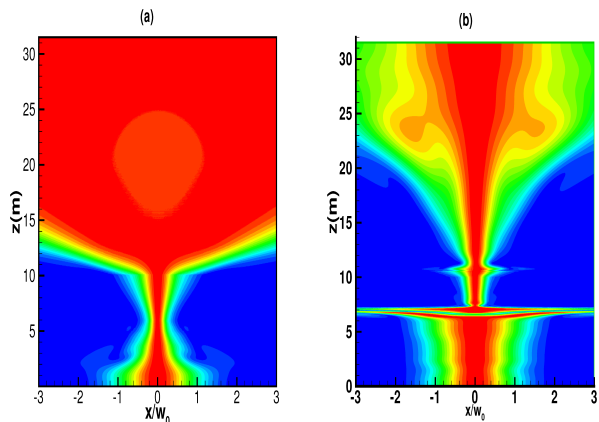
Figure 2: Transverse intensity profile of the fundamental resonance wavelength (a) and the third harmonic wavelength (b) in the x direction for $y = 0$
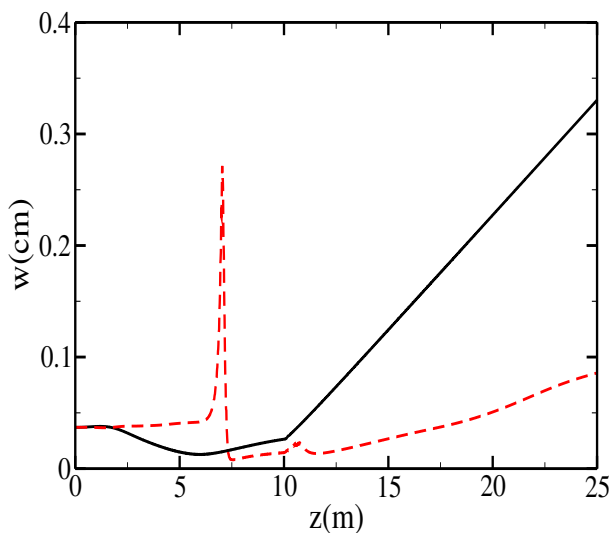

Figure 3: Evolution of the radiation spot size for the fundamental resonance (solid line) and third harmonic (dashed line).

power. The third harmonic wavelength is at 34.5 nm and starts from zero initial power. The initial radiation waists are 0.037 cm and the initial alpha parameters are chosen to be zero. The initial state of electron beams is chosen to model the injection of an axisymmetric electron beams with the flattop density profiles, i.e., $\sigma_\perp = 1$. For unbunched electron beam, the particles are uniformly distributed in phase.

The fundamental resonance is suppressed by reducing the wiggler magnetic field strength at $L_1 = 10$ m with $a_3 = 0.97$ while the third harmonic grows to saturation. In Fig. 1, the power of the fundamental resonance (solid line) and the third harmonic (dashed line) are plotted as a function of the distance through the wiggler. The intensity of the shorter wavelength is larger than the intensity of the fundamental wavelength. Therefore, reducing the wiggler magnetic field, the fundamental resonance will be suppressed and the third
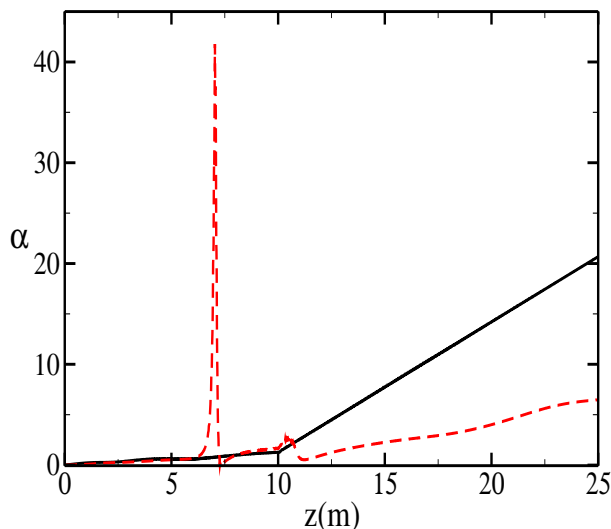

Figure 4: Evolution of α_1 and α_3 with longitudinal coordinate.

harmonic of the first segment of the wiggler is a seed for the fundamental harmonic of the second segment of the wiggler leading to higher power. The fundamental resonance in Fig. 1 is suppressed at $z = 10$ m with the power of 2.7×10^7 W. The third harmonic approaches to saturation point at $z = 19.5$ m with the power of 4.8×10^7 W.

Evolution of the radiation amplitude in the transverse plane is shown in Figs. 2(a) and 2(b) as a function of z for the fundamental mode and the third harmonic, respectively. Although, these figures do not show the amplification of the radiation because of normalization of transverse profile to peak intensity of 1, they show that the amplitude profile of the radiation in the transverse plane becomes narrower as the radiation propagates toward the point of saturation and this mode narrowing is greater for the third harmonic. As it is seen in Fig. 2(b), the transverse intensity profile for the third harmonic initially widens until z=6.6 m, the point where the small gain ends. Because the radiation undergoes diffraction in the small gain region and experiences rapid focusing so-called gain guiding, at the onset of exponential growth it leads to narrowing transverse intensity profile. Thus, the transverse profile of the radiation appears to be guided with an exponentially growing amplitude. The position of the saturation point can be inferred from the point where mode narrowing stops and the intensity profile widens. Because the gain guiding is no longer effective after the saturation point the radiation waist begins to grow.

In Fig. 3, the radiation waist of the fundamental resonance and third harmonic are plotted. The radiation waist for the third harmonic is observed to expand, from its initial size, during the small signal region because of vacuum diffraction. This can also be seen in Fig. 2(b). At the exponential growth region, optical guiding becomes strong and focusing is rapid. Finally, the radiation waist expends rapidly as the saturation point is reached. The radiation waist for the fundamental
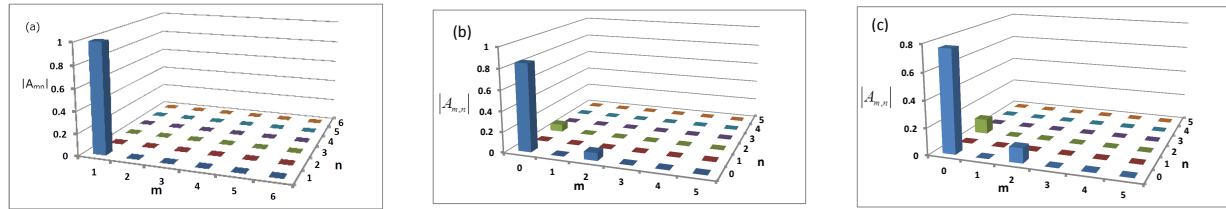
Figure 5: Composition histogram of modes at the beginning wiggler (a), the suppresion point (b), and the saturation point (c).

resonance behaves similar to the third harmonic, and grows faster at the suppressing point.

The curvature of the phase front, α, is shown in Fig. 4. Both fundamental and the third harmonic, which are plane waves at the entrance to the wiggler at $z = 0$, deviate from plane waves as radiation travels along the wiggler. The curvature of the phase front of the third harmonic increases abruptly as saturation occurs but for the fundamental resonance, it increases rapidly at the suppression point.

The composition process will introduce higher-order modes in an attempt to account. Figure 5 shows the mode content histogram at the beginning, suppression and saturation point of the third harmonic. Figure 5 represents that a purely (0,0) mode at the beginning of the wiggler. It can be seen that the lowest order mode $TEM_{0,0}$ is dominant at the saturation point.

CONCLUSION

In this paper, we analyzed harmonic lasing to enhance harmonic generation in the frame work of the realistic 3D model of the FEL process by using a nonaveraged simulations, which is named CYRUS 3D. In the absence of slippage, the variation of radiation waists, curvatures, and amplitudes for fundamental resonance and the third harmonic are studied. The radiation power of the third harmonic is larger than that of the fundamental resonance in contrast to the nonlinear harmonic generation. Also, the composition of significant modes of the third harmonic is presented which shows that the lowest order mode is dominant.

REFERENCES

[1] W. Ackermann, G. Asova, V. Ayvazyan, A. Azima, N. Baboi, Nature Photon. **1**, 336 (2007).

[2] R. Bonifacio, L. De Salvo, and P. Pierini, Nucl. Instrum. Methods Phys. Res., Sect. A **293**, 627 (1990).

[3] H. P. Freund, S. Biedron, and S. Milton, Nucl. Instrum. Methods Phys. Res., Sect. A **445**, 53 (2000).

[4] Z. Huang and K. Kim, Phys. Rev. E **62**, 7295 (2000).

[5] E. L. Saldin, E. A. Schneidmiller, and M. V. Yurkov, Phys. Rev. ST Accel. Beams **9**, 030702 (2006).

[6] B. W. J. McNeil, G. R. M. Robb, M. W. Poole, and N. R. Thompson, Phys. Rev. Lett. **96**, 084801 (2006).

[7] E. A. Schneidmiller and M. V. Yurkov, Phys. Rev. ST Accel. Beams **15**, 080702 (2012).

[8] E. L. Saldin, E. A. Schneidmiller, and M. V. Yurkov, Opt. Commun. **281**, 1179 (2008).

[9] L. H. Yu and J. Wu, Nucl. Instrum. Methods Phys. Res A **483**, 493 (2002).

[10] H. P. Freund, S. G. Biedron, S. V. Milton, IEEE J. Quantum Electron. **36**, 275 (2000).

[11] L. H. Yu and J. Wu, Nucl. Instrum. Methods Phys. Res A **483**, 493 (2002). P. Sprangle, A. Ting, and C. M. Tang, Phys. Rev. Lett. **59**, 202 (1987).

[12] B. Hafizi, P. Sprangle, and A. Ting, Phys. Rev. A **36**, 1739 (1987).

[13] P. Sprangle, A. Ting, and C. M. Tang, Phys. Rev. A **36**, 2773 (1987).

[14] B. Hafizi, P. Sprangle, and J. R. Penano, Nucl. Instrum. Methods Phys. Res.Sect. A **581**, 601 (2007).

[15] A. Chakhmachi and B. Maraghechi, Phys. Plasmas **16**, 043110 (2009).